

Estimation and validation of roughness length, surface temperature and sensible heat flux computed from remote sensing (WiFS and NOAA/AVHRR) data

R. K. GUPTA, T. S. PRASAD AND D. VIJAYAN
National Remote Sensing Agency, Hyderabad - 500 037, India.

ABSTRACT

For computation of Land Surface Processes on regional/global basis for General Circulation Models, a feasible option is the use of satellite data. In this study roughness length was estimated from NOAA/AVHRR data and IRS-1C/WiFS data. Surface temperature and sensible heat flux were estimated from NOAA/AVHRR data. The results were compared with ground/tower-based methods. Roughness length estimated using circular average method with application of fetch distance concept produced good results. Consistency check was performed for estimated surface temperature. Sensible heat flux estimated from NOAA/AVHRR data matched closely with the ground measurements.

Key words: Remote sensing, Roughness length, Surface temperature, Sensible heat flux, NOAA/AVHRR, WiFS

Roughness length (Z_0), surface temperature (ST) and sensible heat flux (SHF) are important land surface process (LSP) inputs for general circulation models (GCMs). For computation of such parameters on regional/global scales, use of satellite data is the feasible option. NOAA/AVHRR provides 1.1 km spatial resolution data sets in visible, near infrared (NIR), middle infrared and thermal infrared spectral regions of electromagnetic radiation (e.m.r.), which can be used to compute roughness length and sensible heat flux. The IRS-1C/WiFS data in 188 m spatial resolution in red and near infrared (NIR) region can also provide an estimation of roughness length at 188 m grid scale. The 36.25 m IRS/LISS II data could also be used to compute the roughness length for micro level diagnostic insights of the processes and to explore answer for the observed singularities.

Vegetation is the dynamic component of

boundary and surface layer characteristics. Satellite based data sets can be utilised in estimating the green biomass using the concept of normalized difference vegetation index (NDVI) with measurements in red/visible and near infrared (NIR) bands. Various types of vegetation indices have been discussed in Deekshatulu and Gupta (1994) and in Bannari *et al.* (1995). NDVI has been used to estimate roughness length (Bolle and Streckenbach, 1993).

MATERIALS AND METHODS

Indian Institute of Tropical Meteorology (IITM), Pune, conducted a Land Surface Processes (LSP) Experiment (LASPEX-97) in Sabarmati river basin. The roughness length Z_0 and sensible heat flux (SHF) computed by IITM from the measurements undertaken at Anand site have been used to compare with the Z_0 and SHF computed from satellite data. Fig. 1 shows the diurnal variation of roughness

length estimated through wind profile method for February 25 and 26, 1997. Roughness length (Fig. 1) is high during dawn and dusk and low during the daytime. In this paper, NDVI was used to estimate roughness length. NDVI does not change over the day. Satellite can provide daytime measurements over an area only once at the time of its pass. NOAA/AVHRR data pertaining to 1330 hrs. local solar time (LST) was used to compute the NDVI and surface temperature and moreover the reflected signal in visible/red and NIR band would be strong around 1330 hrs. Because the equatorial crossing time of IRS and NOAA satellites are 1030 hrs. and 1330 hrs., respectively, Z_0 computed from satellite based NDVI were verified with the estimation of Z_0 made by IITM from tower based measurements undertaken at these respective times. The IRS/WiFS offers diagnostic oriented value addition in obtaining roughness length during the onset of weather development, i.e. at 1030 hrs., as NOAA/AVHRR afternoon ascending pass observations cater to estimation of Z_0 for peak weather development situation (around 1330 hrs.). Availability of thermal IR split window in NOAA/AVHRR data enables estimation of surface temperature at 1330 hrs. LST, which, together with Z_0 , is used for computing SHF.

Data

For the present study, IRS-1C/WiFS data of February 25, 1997 and NOAA/AVHRR data of February 26, 1997 were chosen since the relative comparison of roughness length estimation from NOAA/AVHRR and WiFS could be possible as the vegetation conditions do not change in a day or two. IITM and Gujarat Agricultural University (GAU) have collected extensive ground based meteorological data sets towards LSP studies over the LASPEX region and NRSA had

participated in the collection of spectral, hyperspectral and thermal measurements over several crops towards diagnostic studies of space based measurements. NRSA has also undertaken, at fortnightly interval, ground surveys in Anand-Khandha-Derol region towards (i) ground-truth collection for remote sensing data based land use/land cover classification and (ii) for undertaking regional extension for the estimation of Z_0 and SHF using IITM LSP experiment measurements at Anand, Khandha and Derol.

Estimation of roughness length

Scientists working in LASPEX-97 began to realize the necessity of relating NDVI with roughness length to explore the possibility of estimating Z_0 from satellite data. The Tomelloso (Bolle and Streckenbach, 1993) proposed the following relation:

$$Z_0 = \exp(-5.5 + 5.8 \text{ NDVI}) \quad \dots(1)$$

whereas according to Barrax method,

$$Z_0 = \exp(-5.2 + 5.3 \text{ NDVI}) \quad \dots(2)$$

The NDVI is a parameter, which indicates vegetation biomass level and is defined as

$$\text{NDVI} = \frac{\text{NIR} - \text{Red}}{\text{NIR} + \text{Red}} \quad \dots(3)$$

where NIR and Red are radiances in NIR and red/visible bands, respectively. The normalization through division with the sum of radiances in NIR and red in the equation (3) takes care of atmospheric, scan angle and illumination geometry observation errors at first approximation level. Since roughness lengths derived from these two methods are similar (Fig. 2) and almost merge at higher

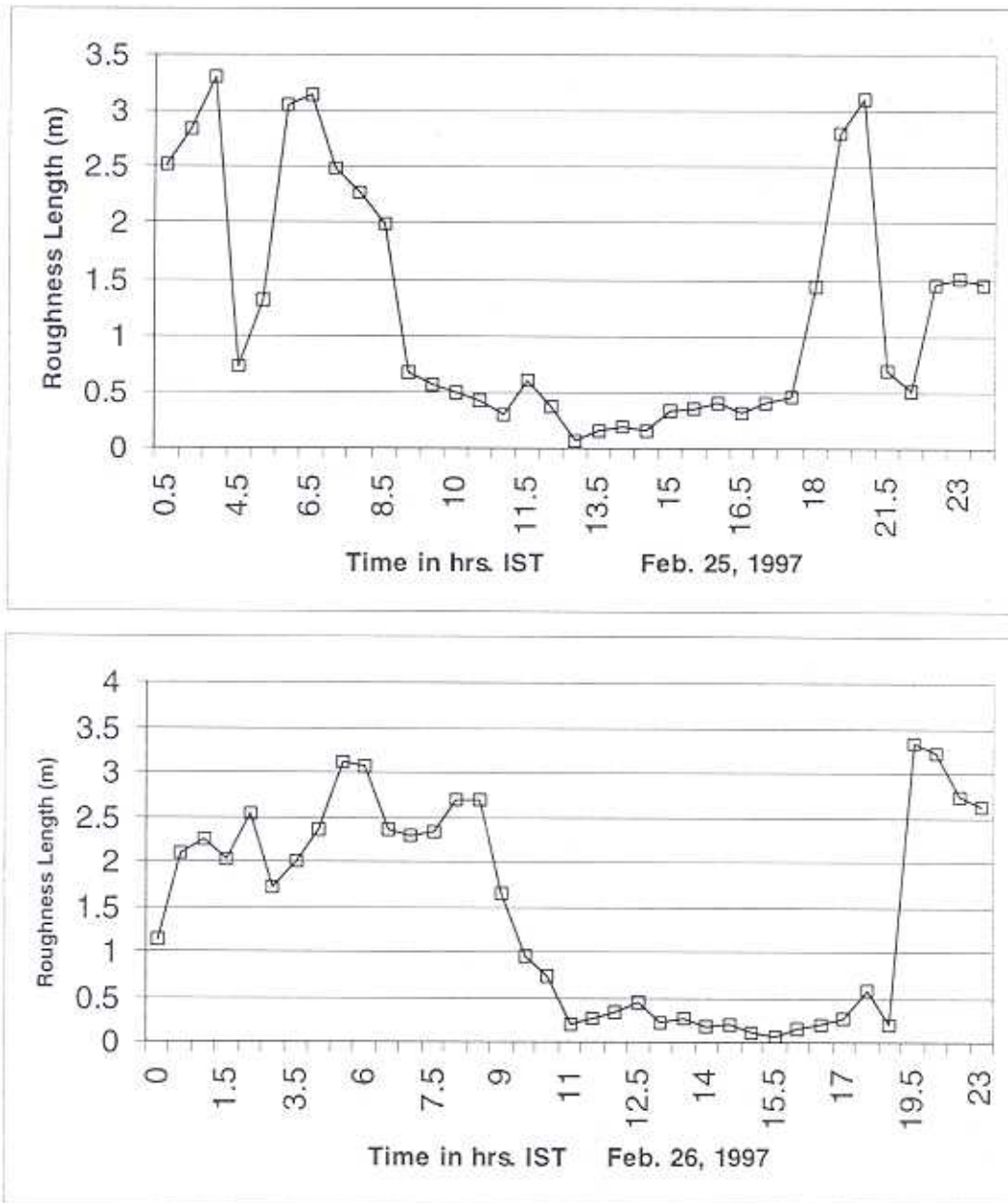


Fig. 1 : Diurnal variation of roughness length derived from wind-profile method for February 25 and 26, 1997 (courtesy: IITM, Pune).

values of NDVI, thus any one of these methods can be used. To develop our own relationships, we would need large coincident data sets from satellite and tower based measurements. In the current study, Tomelloso method was used and it was found that the Z_0 computed from satellite data was always lower than those computed from tower based methods.

To bring the values closer to conventional value, the satellite-based values were scaled by multiplying with eleven. Thus the modified Tomelloso relation as given below

$$Z_0 = 11 * \exp(-5.5 + 5.8 \text{ NDVI}) \quad \dots(4)$$

was used and was found matching well with conventionally measured Z_0 over the Anand region.

The conventional tower based measurements use wind profile method wherein direction as well as speed keeps varying with time. NDVI, computed from satellite data at 1.1 km spatial resolution, would not change with time over the day and perceptible changes may occur at weekly interval. Since the wind field gets modified by the location of vegetation and other obstacles within 100 km radius around the location of tower, the NDVI was computed upto 100 pixels radius circle (taking the pixel covering the tower location as centre) for 1.1 km resolution AVHRR data and upto 600 pixels radius circle for IRS-1C/WiFS (188 m resolution) data.

Computation of average NDVI for the circle would be the simplest approach. To give weightage to prevailing wind direction one could select the 15° sector (i.e., 360 degree domain categorized in 24 sectors)

and use the sector, which encompasses the wind direction at the time of observation. The other option could be to take $\pm 1^\circ$ sector around the wind direction at the time of wind profile measurement. The idea was to assess the comparative aspects of roughness parameter derived from satellite data, by various methods within the zone of influence with the conventional data.

Other dimension of thinking could be that once a high or extensive obstruction from vegetation (for city region, NDVI does not work) stretches its influence on the incoming wind field, thereafter smaller height vegetation (over non-wide horizontal extent) on the down side of the wind would not considerably modify the signatures of already modified wind field. With this in view, the following approaches were adopted:

Method A

Using average NDVI and thereafter calculating Z_0 with increasing pixel range i.e., with increasing distance from tower in

- (i) a circle around the tower location
- (ii) a sector of 15° angle encompassing wind direction at the time of observation
- (iii) sector of 3° (i.e., $\pm 1^\circ$) w.r.to wind direction at the time of observation

In the above methods [i.e., under A], the pixels having very less NDVI values (i.e., < 0.05) were ignored in the estimation of Z_0 .

Method B

Using maximum NDVI (encountered within the range of pixels in a given 15° sector) in the sectors of 15° angle over the circle of influence around tower.

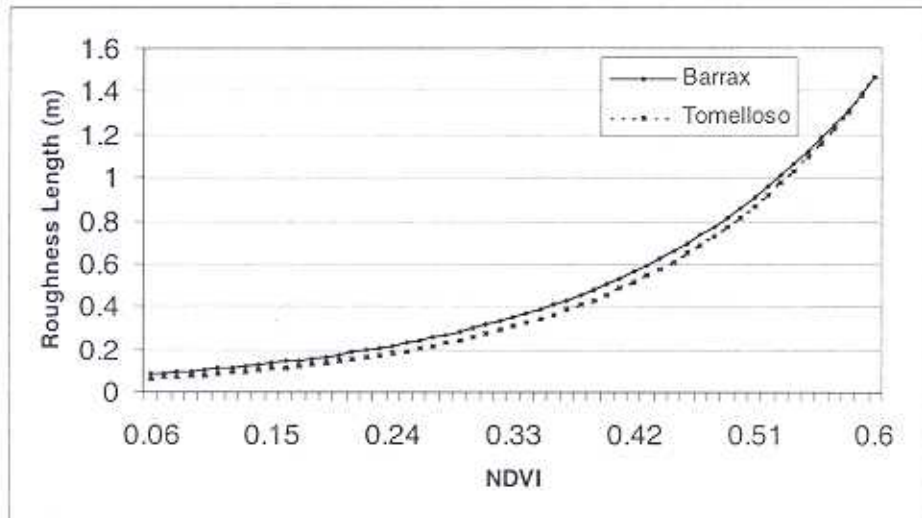


Fig. 2 : Roughness length derived from simulated NDVI by Barrax and Tomelloso methods.

Estimation of land surface temperature

Surface temperature over land and ocean is of undeniable importance in agriculture, meteorology, environmental and other applications. Measurement of surface temperature over land by remote sensing is difficult because of its heterogeneity. This requires knowledge of emissivity of each pixel whose physical (kinetic) temperature needs to be determined. This difficulty has been circumvented with the split window thermal channels provided in NOAA/AVHRR and by using the NDVI in modulating the emissivity variation over the crop growth cycle (CGC).

The emitted radiation is collected in 10.3-11.3 μm (channel 4) and 11.5-12.5 μm (channel 5) of AVHRR and the corresponding brightness temperatures are indicated by T_4 and T_5 , respectively. These two temperatures are used to estimate kinetic temperature (T_{kin}) using split window algorithm (Becker and Li, 1990) as

$$T_{kin} = aT_4 + b(T_4 - T_5) + c \quad \dots(5)$$

where a, b and c are coefficients obtained by statistical analysis.

One usually encounters partially vegetated pixels, especially in 1.1 km resolution AVHRR data. Further, the magnitude of mixed characteristics (relative areal-view based proportion of soil and crop) of the partially vegetated pixel changes as a function of phenological stage of the crop. In such a case NDVI could be used as a surrogate parameter towards assessing the relative contribution of soil and vegetation over CGC during estimation of land surface temperature. Here, one could compute the temperatures T_4 and T_5 under two assumptions, viz., (a) the pixel is totally devoid of vegetation (T_2); and (b) the pixel is totally covered with vegetation (T_1) using equation (6).

$$T_{kin} = A + B (T_4 + T_5)/2 + C(T_4 - T_5)/2 \quad \dots(6)$$

Here A, B and C are functions of emissivity in AVHRR channels 4 and 5, average and

difference of emissivities in these two channels. While computing the T_g , the emissivities corresponding to soil in channels 4 and 5 were used (Becker and Li, 1990) and during computation of T_v the emissivities corresponding to maximum NDVI were used. The NDVI for bare soil ($NDVI_{soil}$) and full canopy ($NDVI_{veg}$) and the corresponding emissivity values, used in computing T_g and T_v are available in Becker and Li (1990).

Now the relative mix-up for vegetation component ($NDVI_n$) for the given pixel could be estimated using

$$NDVI_n = \frac{NDVI_{(pixel)} - NDVI_{soil}}{NDVI_{veg} - NDVI_{soil}} \quad \dots(7)$$

The kinetic temperature of the pixel could be computed using

$$T_{kin} = NDVI_n T_v + (1-NDVI_n) T_g \quad \dots(8)$$

Details of this methodology are available in Gupta *et al.* (1997).

Estimation of sensible heat flux

An attempt has been made to derive sensible heat flux from NOAA/AVHRR data and to compare the same with the one obtained by tower data-based method in the LSP experiment conducted by IITM.

Equation for sensible heat flux (H) can be written as (Bolle and Streckenbach, 1993; Chehbouni *et al.*, 1997; Vining and Blad, 1992)

$$H = \frac{\rho C_p (T - T_a)}{r} \quad \dots(9)$$

where ρ is air density, C_p is specific heat of air at constant pressure, T and T_a are temperature of pixel and air, respectively. r is aerodynamic resistance to sensible heat flux defining

exchanges within the surface layer and can be calculated using the following relationship given by Bolle and Streckenbach (1993)

$$r = \frac{1}{u^*k} \ln \frac{Z}{Z_0} \quad \dots(10)$$

where k is Von Karman constant (~ 0.41), Z is height of measurement, Z_0 is roughness length and u^* is friction velocity. Equation (9) is valid when vertical transport of heat and momentum become much larger than horizontal transport (Hall *et al.*, 1992).

RESULTS AND DISCUSSION

Roughness length was obtained using the NDVI derived from NOAA/AVHRR as well as IRS-1C/WiFS data using the approaches mentioned in the section named "Estimation of roughness length". The AVHRR radiances were corrected for sensor degradation (Rao and Chen, 1996), atmospheric (Rayleigh) scattering and scan angle effects using dark body method and thereafter equation (3) was used to compute NDVI. Fig. 3 shows the comparison between uncorrected and corrected NDVI wherein one can realise the necessity of corrections for sensor degradation and atmospheric effects. Here X-axis refers to distance in pixels in tower location and Y-axis refers to NDVI computed by circular averaging the NDVI values with tower location as the centre.

Spatial distribution of roughness length in WiFS and AVHRR images

For WiFS data, the digital count values were converted into radiance measurements (using sensor gain and offset values) prior to computing the NDVI. WiFS collects data in 0.62-0.68 μm (red) and 0.77-0.86 μm (NIR) bands. Plate 1 gives the IRS WiFS image

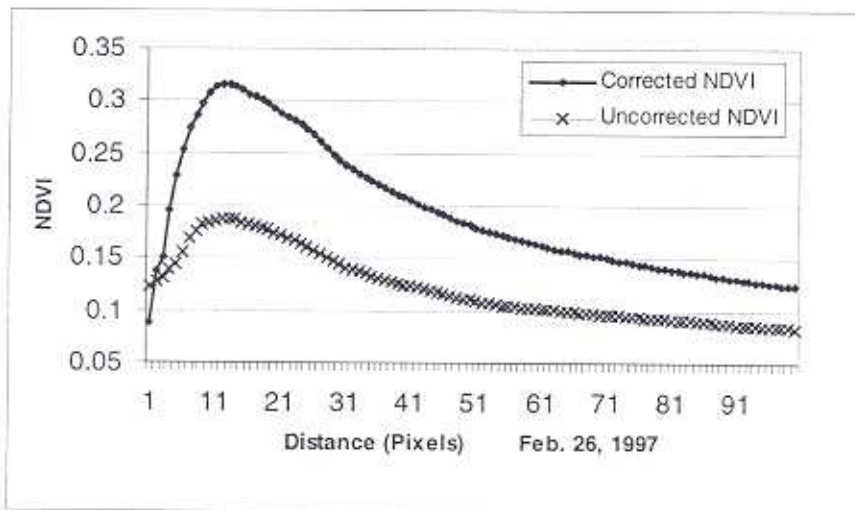


Fig. 3 : Comparison between atmospherically corrected and uncorrected NDVI of NOAA / AVHRR data.

where agriculture areas are seen in varying degrees of red shades.

The use of NDVI for roughness length estimation is justified, as the increased magnitude of vegetation would create more surface roughness for the wind field. Higher the NDVI, higher the vegetation under the pixel, hence more interaction with the wind field which will result in increased Z_0 .

Plates 2 and 3 show NDVI derived from IRS-1C/WiFS data (February 25, 1997) and NOAA/AVHRR (February 26, 1997), respectively. Plate 4 & 5 show the roughness length images derived from IRS-1C WiFS and NOAA/AVHRR respectively. One could locate Anand city in plates 2 and 4 with the help of annotation in plate 1. The small black portion in near centre of plate 2 indicates predominant concrete component of city

while the blue component around this black portion refers to near periphery zone of the Anand city and the crimson (NDVI in 0.05-0.10 range) around blue refers to outskirts boundary of the Anand city. In WiFS roughness image Z_0 for NDVI values upto 0.05 are getting merged giving $Z_0 < 0.05$ m, which may not be realistic. To take care of city zone, the city category specific Z_0 had to be independently incorporated with computed Z_0 from NDVI image over non-city zones to get realistic spatial distribution of Z_0 , which will also modify the aggregated value for Z_0 . This could be achieved using Geographic Information System (GIS). In WiFS roughness image (plate 4), Z_0 in range of 0.05 - 0.10 predominantly encompasses three (< 0.00, 0.00 - 0.05 and 0.05 - 0.10) ranges of NDVI (plate 2) with some pixels (near NDVI value of 0.10) getting placed in

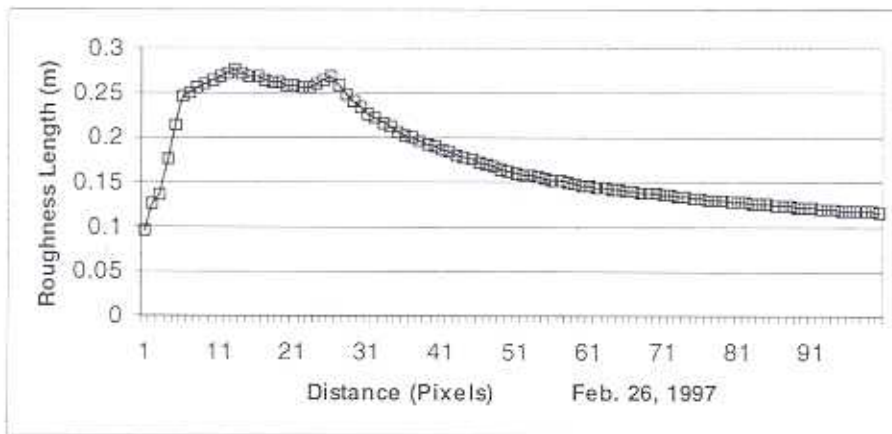


Fig. 4 : Variation of roughness length as a function of distance from tower (in terms of number of NOAA/AVHRR pixels) for method A(i), i.e., circular averaging.

Z_0 range of 0.10 -0.15 m. For inner river water and highly concrete zones one expects $NDVI < 0$. At very high $NDVI$ ranges i.e. 0.45 - 0.50 and 0.50 - 0.58 (plate 4), Z_0 is getting into single category in plate 4 for the reason that the range for Z_0 is wide (0.95 to 1.30) -- kept for the sake of limitation in the perceptive capability for analysis of colour coded images. In between the stages, it is seen that geometric structures are easy to perceive in Z_0 image as compared to that in $NDVI$ image.

Plate 6 represents the AVHRR image over the region in near IR band where increasing intensity in the agriculture region appears in increasing degree of whiteness. Water bodies appear black while urban and semi-urban regions appear in bluish grey shade. The city of Anand is located below the annotation. Since AVHRR data is in 1.1 km resolution, the descriptions cannot be handled in the way it had been for WiFS (188 m spatial resolution) images (plates 1, 2 and 4). Since

the mixedness (in pixel) would be large for 1.1 km resolution pixel as compared to that for 188 m resolution pixel, the upper limits of $NDVI$ (0.52 for AVHRR, 0.58 for WiFS) and Z_0 (0.92 for AVHRR, 1.30 for WiFS) for AVHRR are lower as compared to that for WiFS data. Objects with $NDVI$ in <0.0 to 0.05 range (plate 3) are getting merged in $Z_0 < 0.05$ range (plate 5) as was the case for WiFS. Smoothness in transition as observed in $NDVI$ image is not perceptible in Z_0 image as Z_0 is the negative exponential function of $NDVI$. The examination of the numerical data pertaining to the plates 1 to 4 revealed that the $NDVI$ as well as roughness length over built up areas, from satellite data, is low. This can be inferred particularly from Plate 4. Therefore, one limiting factor with the roughness length estimation through $NDVI$ method is that it can be employed only over vegetative covered areas. The varying aspects of agricultural activities around Anand city are getting reflected in $NDVI$ as well as Z_0 images.

Table 1 : Sector-wise peak roughness length and its occurrence in terms of AVHRR pixel distance from tower location

Sector (deg.-deg.)	Distance (AVHRR pixels)	Roughness Length(m)	Sector (deg.-deg.)	Distance (AVHRR) pixels	Roughness Length (m)
0-15	21	0.2878	180-195	22	0.4306
15-30	20	0.2789	195-210	23	0.4752
30-45	12	0.3008	210-225	23	0.4537
45-60	12	0.3480	225-240	22	0.4382
60-75	12	0.3431	240-255	25	0.3540
75-90	14	0.3654	255-270	18	0.3580
90-105	13	0.3488	270-285	17	0.3872
105-120	10	0.3043	285-300	14	0.4132
120-135	11	0.3147	300-315	17	0.4067
135-150	12	0.3085	315-330	16	0.3842
150-165	13	0.3447	330-345	15	0.2730
165-180	18	0.3599	345-360	22	0.2558

Estimation of average/representative roughness length

Use of NOAA/AVHRR data

Method A

Conventionally, roughness length is calculated using logarithmic wind profiles and these measurements represent the effect of surface roughness extended over larger distance (fetch distance) which itself is a function of wind speed and degree of surface roughness. Variability of wind direction makes it necessary to average symmetrically in all the directions as a first approximation. From AVHRR data, the NDVI is computed using broad-band 0.55-0.68 μm (visible) and 0.725-1.1 μm (NIR) channels. In case of NOAA/AVHRR data, the maximum radius/fetch distance considered was upto 100

pixels from the tower location and for the IRS-1C WiFS data upto 600 pixels. Roughness length was estimated using NOAA/AVHRR data of February 26, 1997.

Method A(i)

Fig. 4 shows a graph between radius in units of pixels with tower location at the centre and the Z_0 derived from corrected NDVI. The roughness length shows an increasing trend upto radius of 13 pixels and thereafter decreases because of pixels of low vegetation conditions in the circle around the tower. Roughness length at 1330 hrs. estimated from NDVI (0.2811 m) matched well at the radius of 13 pixels with the tower-based calculation of Z_0 (0.2692 m). This may be due to the fact that when the wind interacts with the earth surface features, the features

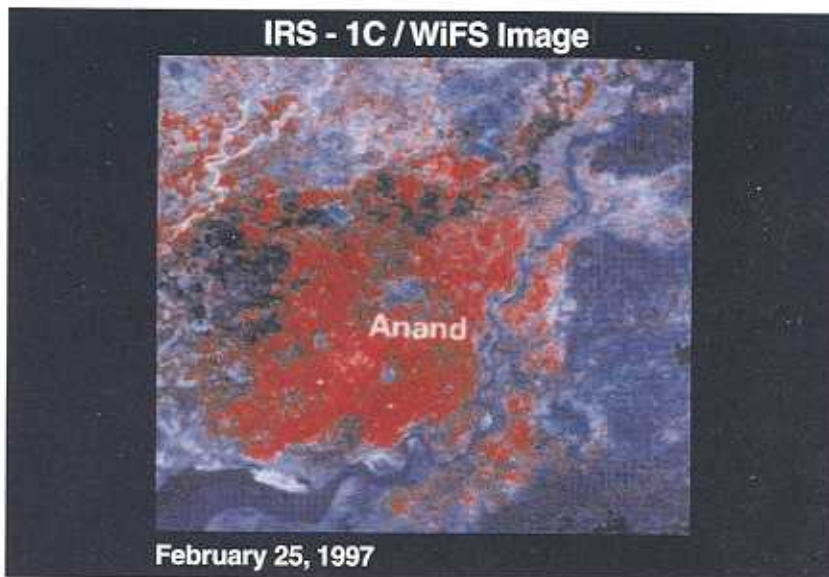


Plate 1 : IRS - 1C / WiFS colour image composite of February 25, 1997 showing Anand and surroundings

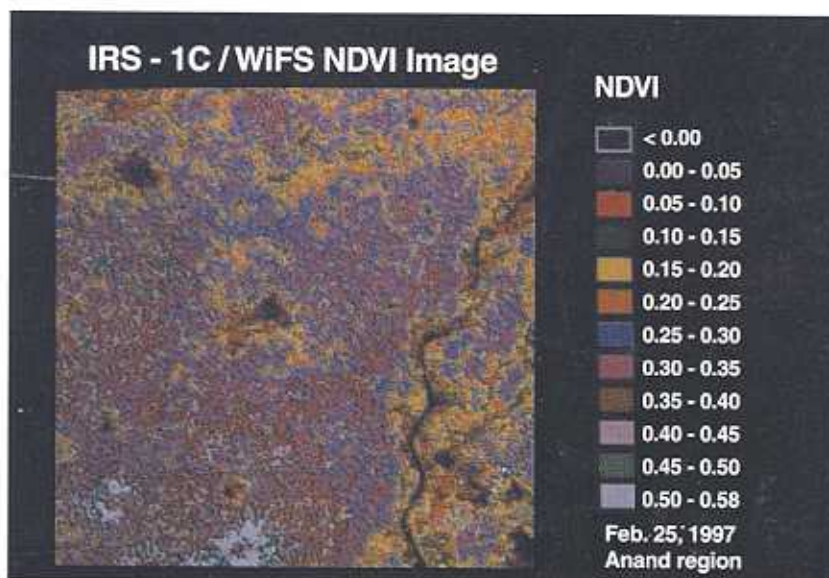


Plate 2 : Colour coded NDVI image derived from IRS - 1C / WiFS (February 25, 1997) covering Anand and surroundings

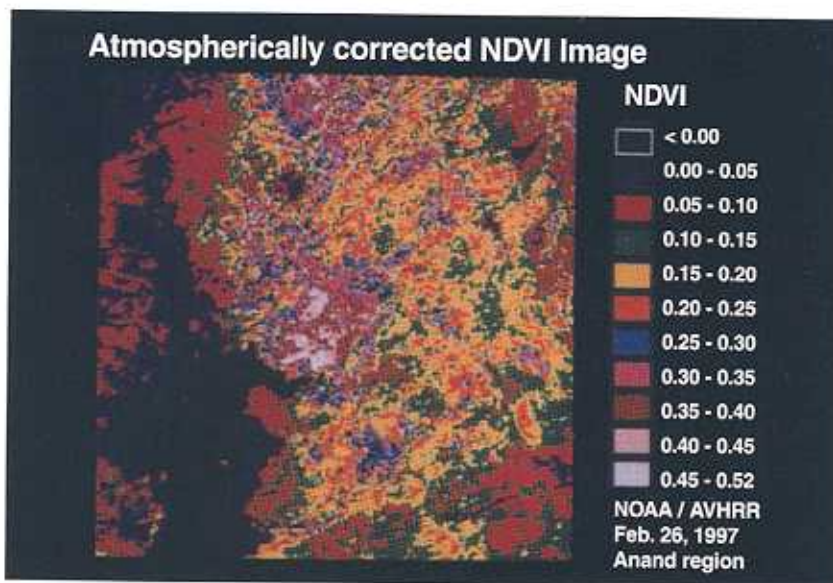


Plate 3 : Colour coded NDVI image derived from NOAA / AVHRR (February 26, 1997) covering Anand and surroundings

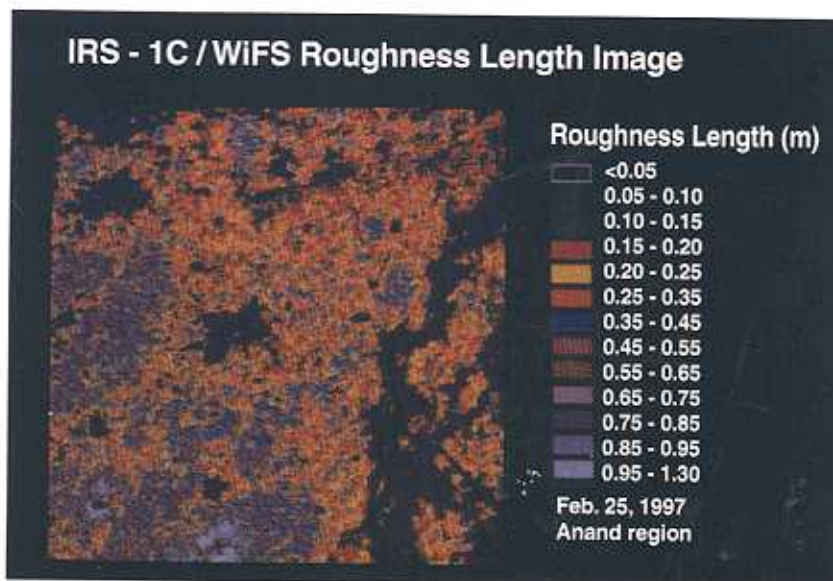


Plate 4 : Roughness length image derived from IRS - 1C / WiFS (February 25, 1997) for Anand and surroundings

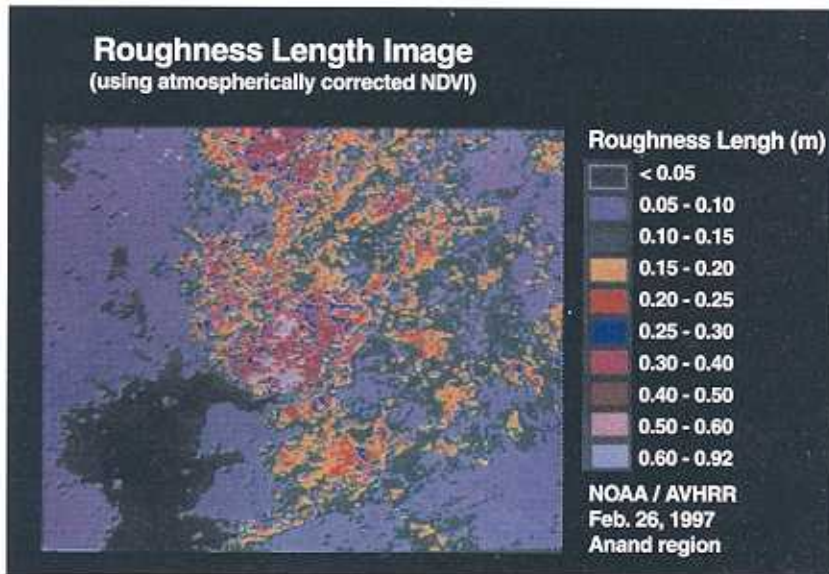


Plate 5 : Roughness length image derived from NOAA / AVHRR data (February 26, 1997) for Anand and surroundings

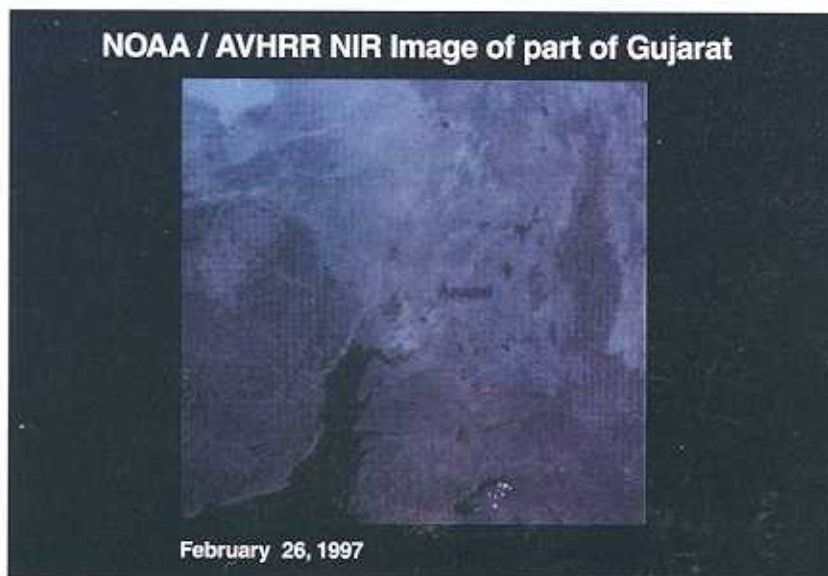


Plate 6 : Near - Infrared band (Band 2) image of NOAA / AVHRR of February 26, 1997 showing Anand and surrounding areas.

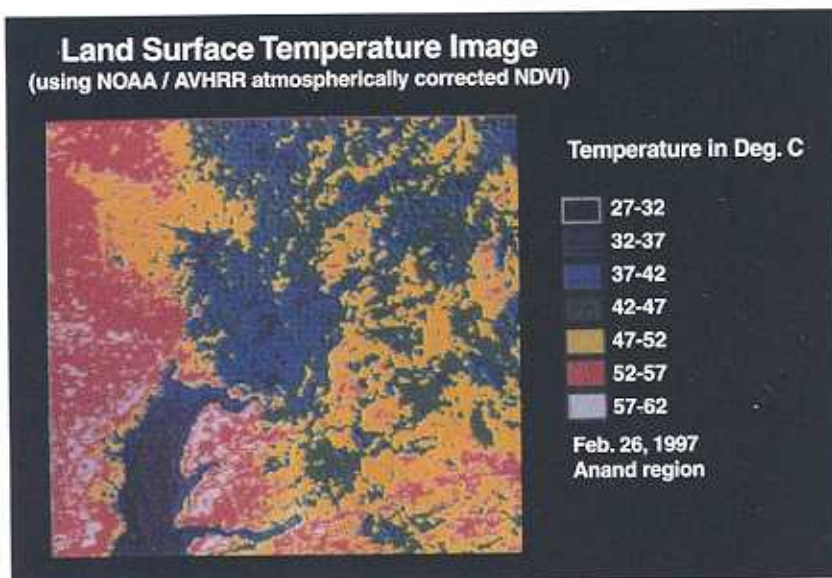


Plate 7 : Surface temperature image derived from NOAA / AVHRR data for February 26, 1997.

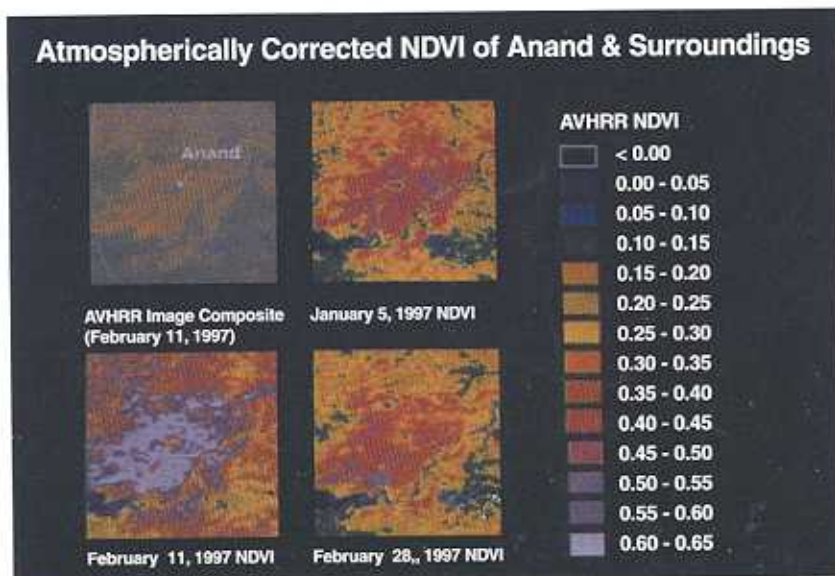


Plate 8 : NDVI derived from NOAA / AVHRR data for January 5, 1997, February 11, 1997 and February 28, 1997.

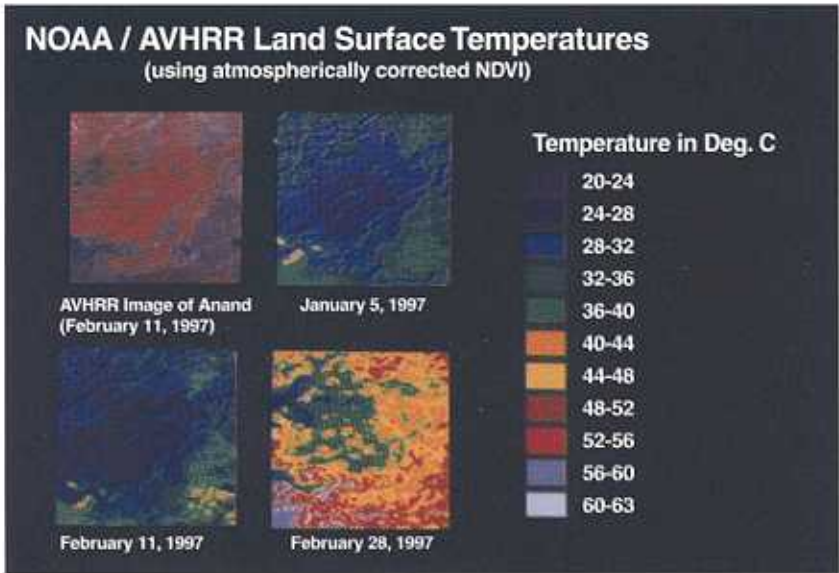


Plate 9 : Surface temperature derived from NOAA / AVHRR data three dates January 5, 1997, February 11, 1997 and February 28, 1997.

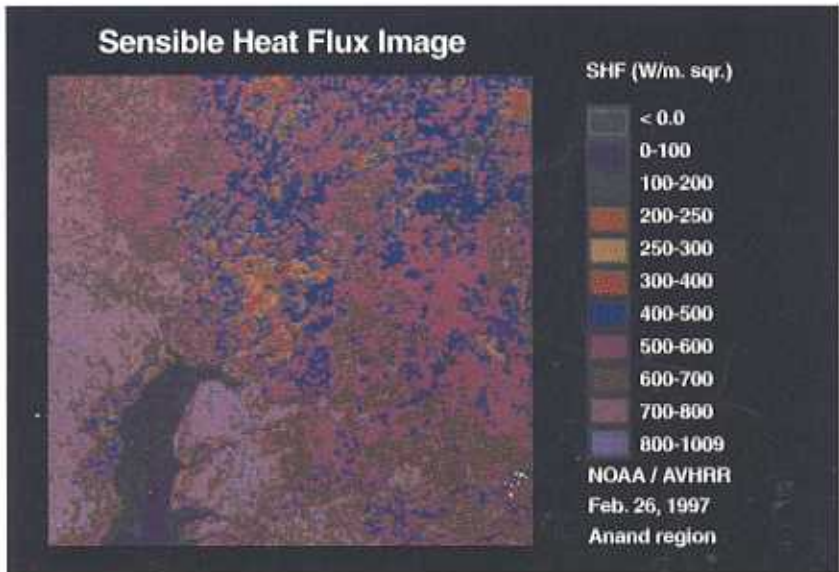


Plate 10 : Sensible Heat Flux image derived from NOAA/AVHRR data for February 26, 1997 over Anand region.

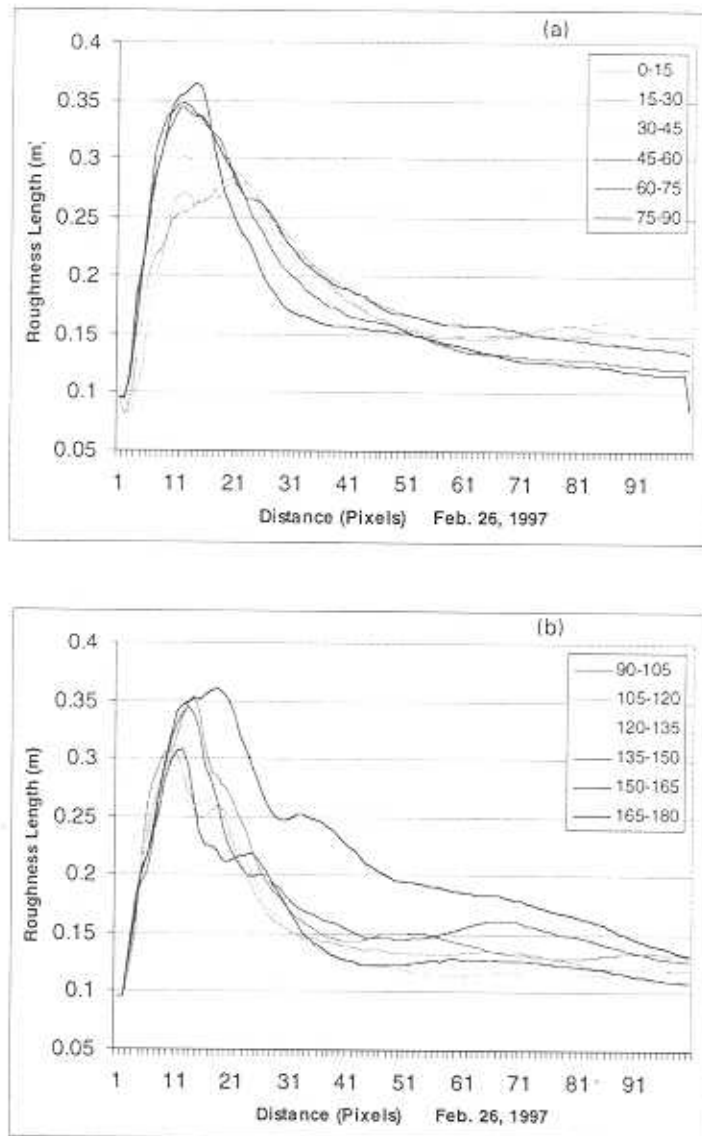


Fig. 5 : (a) and (b). Variation of roughness length as a function of distance from tower (in terms of number of NOAA / AVHRR pixels) for method A(ii), i.e., sector-wise averaging for quadrant: (a) 0° to 90° and (b) 90° to 180° .

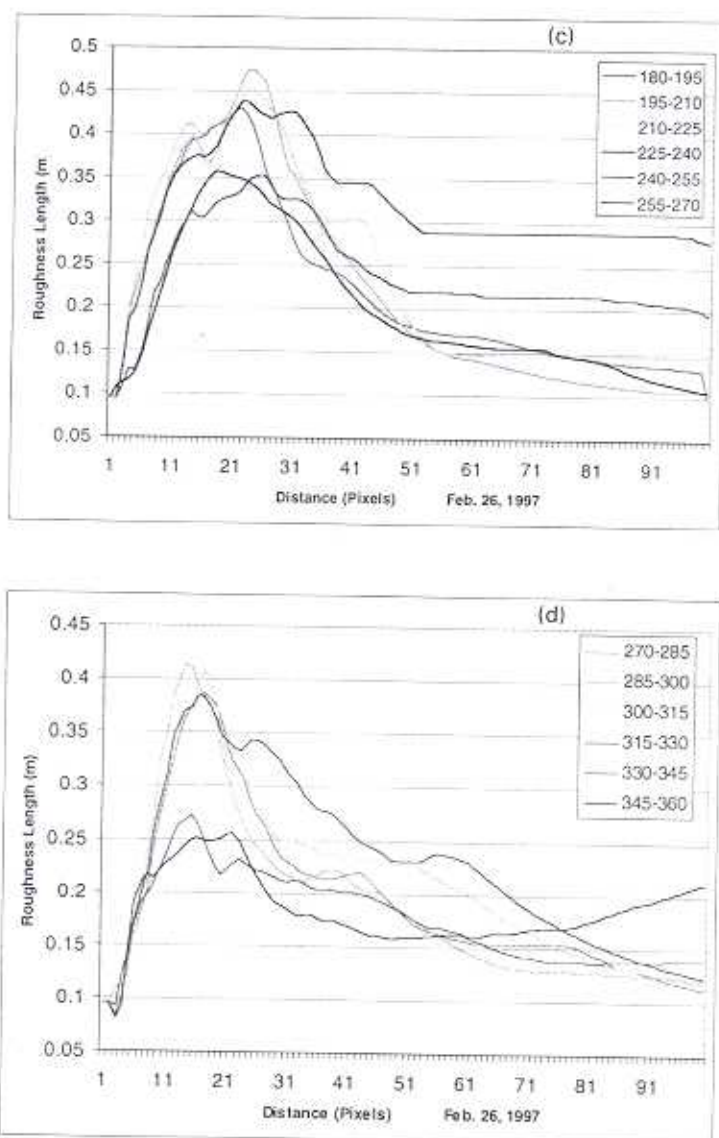


Fig. 5 : (c) and (d). Variation of roughness length as a function of distance from tower (in terms of number of NOAA / AVHRR pixels) for method A (ii) i.e., sector-wise averaging for quadrant: (a) 180° to 270° and (b) 270° to 360°.

Table 2: The least distance in terms of AVHRR pixels in various 15° sectors at which the roughness length from NOAA/AVHRR data came as near as possible with the wind profile-based Z_0 value of 0.2692 m (1330 hrs.).

Sector (deg.-deg.)	Distance (AVHRR pixels)	Roughness Length(m)	Sector (deg.-deg.)	Distance (AVHRR pixels)	Roughness Length (m)
0-15	17	0.2698	180-195	8	0.2699
15-30	12	0.2697	195-210	8	0.2685
30-45	8	0.2619	210-225	7	0.2751
45-60	6	0.2655	225-240	8	0.2669
75-90	5	0.2605	255-270	12	0.2643
90-105	6	0.2614	270-285	11	0.2684
105-120	14	0.2620	285-300	10	0.2702
120-135	8	0.2678	300-315	11	0.2754
135-150	9	0.2812	315-330	10	0.2559
150-165	9	0.2670	330-345	15	0.2670
165-180	9	0.2671	345-360	23	0.2557

closer to the observation location (i.e., the tower) are likely to have more influence/contribution than that from the pixels far away.

Method A(ii)

With reference to North, sectors with angular width of 15° and radii upto 100 pixels covering full circle (0°-15°, 15°-30°, etc.) were independently taken. For these sectors, average NDVI was computed for each radius in steps of 1 pixel from tower location, and the corresponding roughness length was derived. This (roughness length) is shown in fig. 5 'a' through 'd'. As seen here, the sector 165-180° has a widespread peak giving a feeling of multimode with high values of Z_0 falling at 10 to 24 pixels away from the tower.

Thus the incoming wind would get obstructed/modulated over a wide region unlike in other sectors.

Table 1 gives sector-wise peak roughness length and its occurrence in terms of AVHRR pixel distance from tower location. Except for sectors having wider spatial spread of Z_0 with high NDVI values, as mentioned earlier, Z_0 for the other sectors were in the range of 0.2557-0.3546 m. Here again, for sectors 330-345° and 345-360°, the spread was little and peak average NDVI values were the lowest among the 24 sectors. The afternoon wind direction was 27° for which the NDVI based roughness value is 0.2697 m in 15-30° sector. This compared well with the tower-based

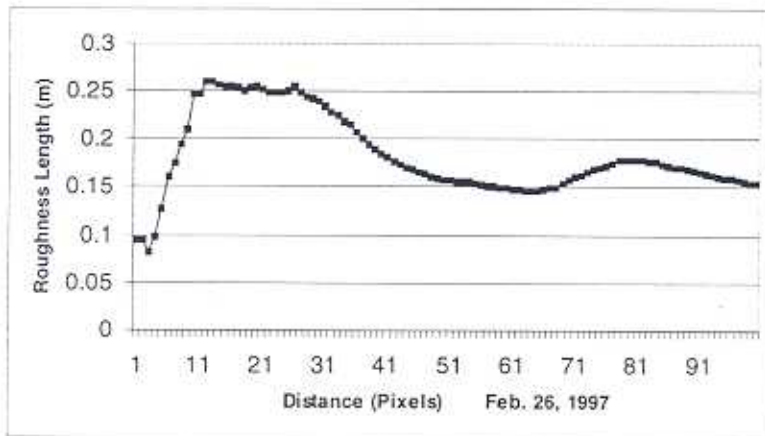


Fig. 6 : Variation of roughness length as a function of distance from tower (in terms of number of NOAA/AVHRR pixels) for method A(iii), i.e., $\pm 1^\circ$ with respect to wind direction (27°).

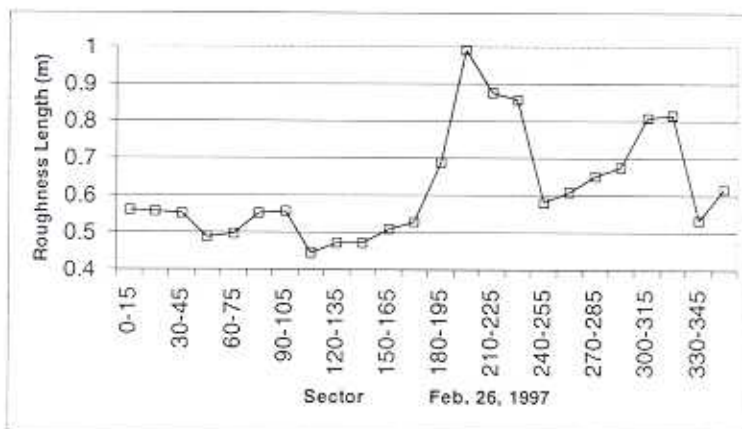


Fig. 7: Variation of roughness length derived using maximum NOAA/AVHRR NDVI within sectors.

value of 0.2692 m.

Table 2 gives the least radius for which roughness length came as near as possible with the wind profile based $Z_0 = 0.2692$ m.

The purpose of this exercise is to provide diagnostic insights for various ways of looking at the contribution of vegetation to Z_0 . The prevailing wind direction at 1330 hrs. was 27° . One can see a near-plateau region in this

Table 3: Sector-wise peak roughness length and its occurrence in terms of WiFS pixels from the tower location

Sector (deg.-deg.)	Distance (WiFS pixels)	Roughness Length(m)	Sector (deg.-deg.)	Distance (WiFS pixels)	Roughness Length (m)
0-15	51	0.3209	180-195	138	0.4964
15-30	43	0.3313	195-210	144	0.4050
30-45	52	0.3072	210-225	158	0.4338
45-60	35	0.3464	225-240	157	0.3659
60-75	62	0.3237	240-255	128	0.3158
75-90	49	0.2824	255-270	117	0.3443
90-105	60	0.3105	270-285	105	0.3620
105-120	60	0.3091	285-300	119	0.3829
120-135	65	0.2721	300-315	86	0.2873
135-150	72	0.3299	315-330	101	0.2405
150-165	58	0.3209	330-345	87	0.2431
165-180	127	0.3907	345-360	60	0.2706

sector over 10 to 34 pixel range. It looks that effect of peak roughness is restricted to 5 to 25 AVHRR pixels from the tower location (Table 2) depending upon the prevailing vegetative and wind conditions.

Method A(iii)

Wind-direction data were taken from the GAU Observatory. A narrow sector of 3° ($\pm 1^\circ$) along the wind-direction was overlaid on the image and average NDVI as a function of radius from tower location was calculated and these average NDVI values were used to compute roughness length. Fig. 6 shows the graph between distance from the tower location and Z_0 . The peak value of roughness length at a radial distance of 13 pixels matched

well (0.2604 m) with the conventionally measured value of 0.2692 m. Here, the Z_0 had near-plateau in the range of radial distance 10-24 pixels. This disables the defining of peak. Thus the matching of Z_0 by this method and wind profile based method at 13th pixel does not seem to be realistic.

Method B (using maximum NDVI)

Within each sector described in A(ii) above, the pixel having maximum NDVI in the sectors of 100 pixel radii was used in roughness length estimation. Figure 7 shows the graph between distance from the tower location and Z_0 . This method overestimates roughness length when compared with the wind profile based estimation of Z_0 .

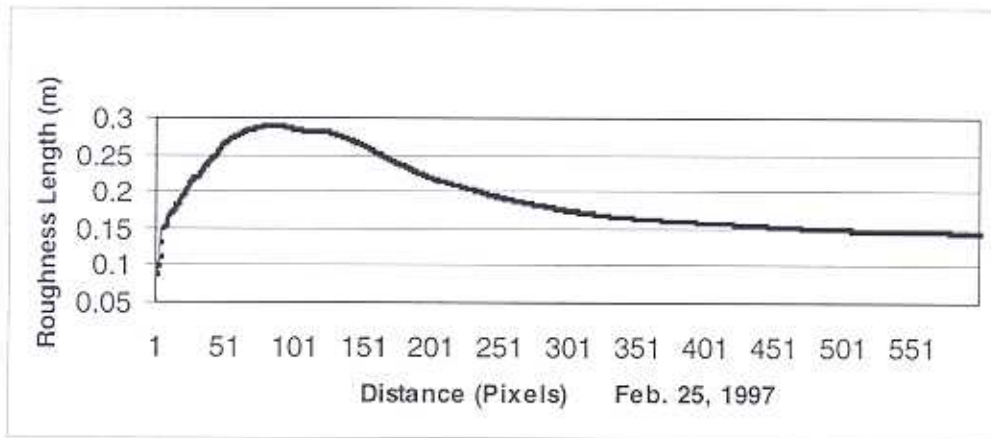


Fig. 8 : Variation of roughness length as a function of distance from tower (in terms of number of IRS-1C/WiFS pixels) for method A(i), i.e., circular averaging

Use of WiFS Data

Method A(i)

Fig. 8 shows the graph between distance from tower location in units of IRS-1C/WiFS pixels and the roughness length. The first mode ($Z_0 = 0.2893$) of the curve was located at the abscissa of 86. This value matches well with the wind profile measurement (0.2972 m). The distance from the tower location for maximum Z_0 value in WiFS data matches well with that for AVHRR data based Z_0 under method A(i) and thus provides reliability to this method.

Method A(ii)

Fig. 9 'a' through 'd' shows the graph between distance from tower location in terms of WiFS pixels and the roughness length. Table 3 gives the summary of the highest value of Z_0 encountered and the corresponding pixel from the tower location for each 15° sector with reference to north.

In the first quadrant ($0-90^\circ$) the maximum Z_0 value occurred at relatively short distance (49 to 62 pixels) as compared with that in the third ($180-270^\circ$) quadrant (117 to 158 pixels). This is because the thick and nearly homogeneous cover of vegetation (mostly tobacco and banana) was located far off in the third quadrant (south-west) and the values of Z_0 were in 0.32-0.50 m range. The values in the first quadrant were in the range of 0.28 to 0.35 m. The peak values of roughness length in the second quadrant were in the range of 0.27-0.39 m. The highest value of Z_0 in this quadrant is 0.39 m, for the $165-180^\circ$ sector where coverage included a part of the tobacco and banana fields. The fields could be seen in Plate 1 in the south and southeast of Anand region.

In the fourth quadrant, the values of Z_0 were usually lower (the exceptions are the sectors $270-285^\circ$ and $285-300^\circ$). This is due to the fact that a considerable number of pixels without much vegetation cover happened to

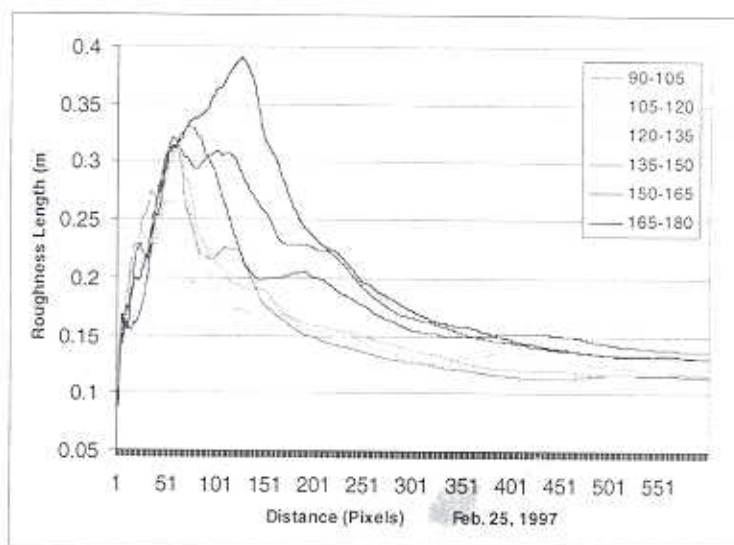
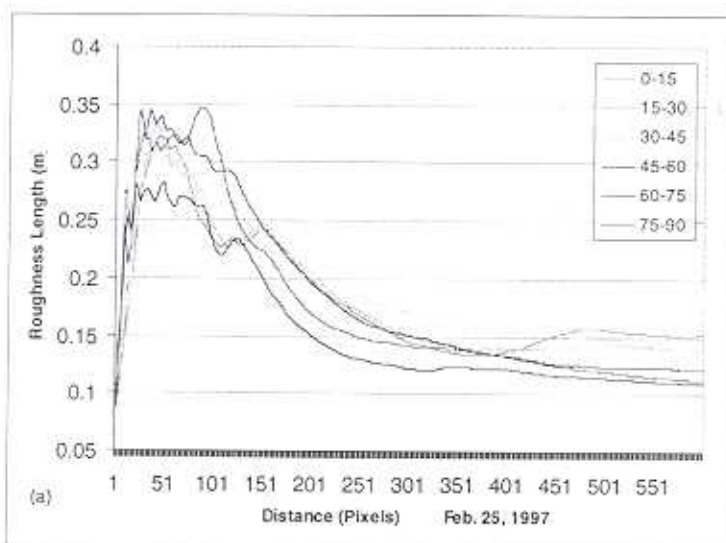


Fig. 9 : (a) and (b), Variation of roughness length as a function of distance from tower (in terms of number of IRS-1C/WiFS pixels) for method A(ii), i.e., sector-wise averaging for quadrant: (a) 0° to 90° and (b) 90° to 180°.

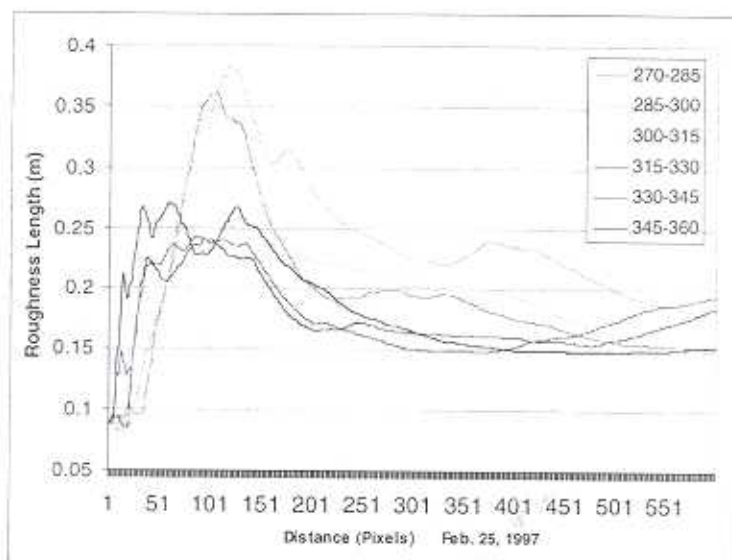
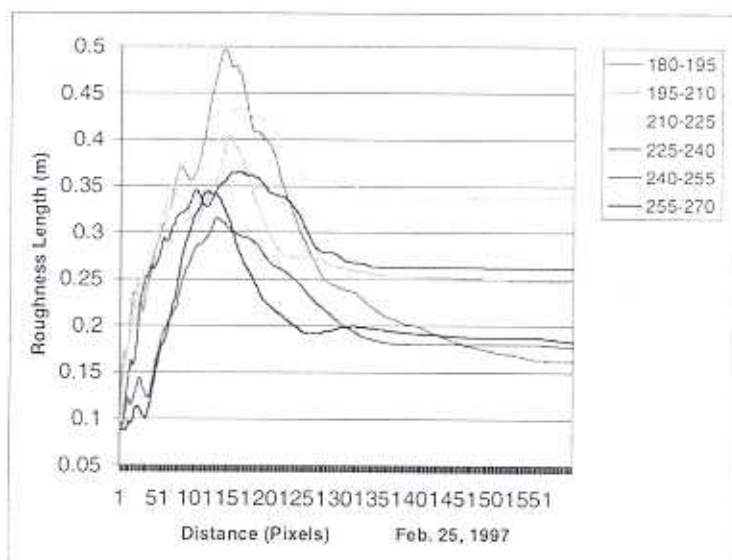


Fig. 9 : (c) and (d), Variation of roughness length as a function of distance from tower (in terms of number of IRS-1C/WiFS pixels) for method A(ii), i.e., sector-wise averaging for quadrant: (c) 180° to 270° and (d) 270° to 360°.

be located in the sectors giving Z_0 in 0.24-0.29 m range.

The ratio of spatial resolution of AVHRR (1.1 km) and WiFS (188 m) is 5.85. The distances for occurrences of peak Z_0 in Table 1 (for AVHRR) and Table 3 (for WiFS) were having considerable mismatch besides having widespread near peak region. This indicates less reliability of this method.

Method A(iii)

Fig. 10 shows a graph between distance from the tower location in units of pixels and roughness length. Here, the Z_0 has been estimated by taking into account the wind recorded by the meteorological observatory. The first mode of the curve is around 44 pixels and the value of Z_0 is 0.3187 m which compares with the tower based Z_0 value of 0.2972 m. The location of first mode in Z_0 in the case of AVHRR (Fig. 6) was at 12th pixel and this does not match with the 44th pixel location in WiFS. Further, wide spectral distribution was observed for near mode values, which makes the mode ill defined in the case of WiFS. Hence this method is not reliable. The circular average method [A(i)] is found more reliable.

Method B

Fig. 11 shows roughness length derived from maximum NDVI value in different 15° sectors. It was found that this method overestimated Z_0 when compared with Z_0 computed from tower based meteorological measurement corresponding to 1030 hrs. (time of observation for WiFS data).

Estimation of surface temperature from NOAA/AVHRR Data

As discussed earlier, for estimation of

surface temperature (ST) over vegetation, NDVI could be used as a surrogate parameter for modulating variation in emissivity over crop growth cycle. Here also, NDVI computed from NOAA data takes into account the correction for sensor degradation, atmospheric scattering and scan angle effects. Temperature of pixel encompassing the tower location in 1.1 km x 1.1 km pixel was estimated as 313.1 K. Plate 7 shows ST image of Anand region derived from NOAA/AVHRR on February 26, 1997 at 1330 hrs., the time of NOAA satellite pass. As expected, the temperature is lower in intensive agriculture areas as compared to those over the barren areas.

Plates 8 and 9 show NDVI image and surface temperature of Anand region for three dates (Jan. 5, Feb. 11 and Feb. 28, 1997). These dates correspond to vegetative stage (Jan. 5, 1997), reproduction stage (Feb. 11, 1997) and senescence stage (Feb. 28, 1997) of the crops. A glance at Plate 8 shows that the NDVI around Anand city is very high on Feb. 11, 1997 image (shown in grey and white colours) indicating the healthy and fully-grown status of crops because of intense agriculture practice. NDVI of pixels pertaining to city zone of Anand (colour coded in green surrounded by yellow in the centre) did not produce perceptible changes from Jan. 5 to Feb. 28, 1997. NDVI of pixels situated at adjacent right of Anand city increased from Jan. 5 to Feb. 11, 1997 and then decreased back on Feb. 28, 1997, indicating that crops moved to maturity/senescence stage.

The surface temperature of the Anand city (shown in green colour at the centre on Jan. 5, 1997 in Plate 9) did not change perceptibly from Jan. 5, 1997 to Feb. 11, 1997. This may be due to the influence of crops around the

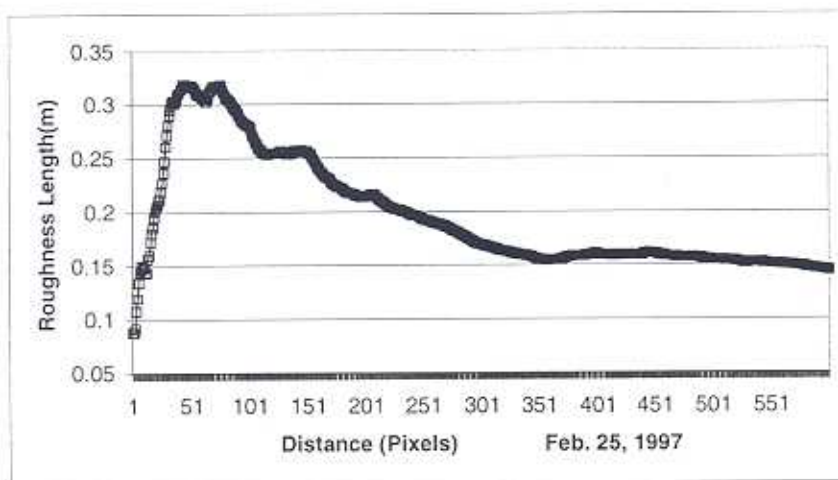


Fig.10 : Variation of roughness length as a function of distance from tower (in terms of number of IRS-1C/WiFS pixels) for method A(ii), i.e., $\pm 1^\circ$ with respect to wind direction (27°).



Fig.11: Variation of roughness length derived using maximum IRS-1C/WiFS NDVI within 15° sectors.

Table 4: Comparison of conventional 1430 hrs. temperature observations with NOAA/AVHRR derived surface temperature (ST) during January/February, 1997

Temperature Measurements	January 5	February 11	February 28
Soil temperature at 2 cm depth	43°C	44°C	45.3°C (surface)
NDVI derived from AVHRR	0.385	0.400	0.254
Crop temperature	21°C	26.1°C (Feb. 12)	32.4°C (Feb. 26)
NOAA/AVHRR ST	28.8°C	30.1°C	43.3°C (Feb. 28) 40°C (Feb. 26)
Air temperature	27.2°C	27.5°C	36.5°C (28 th), 33°C (26 th)
Soil temperature at 5 cm depth	32.5°C	36°C	45.3°C
Soil temperature at 10 cm depth	24.9°C	26°C	32.9°C
Soil temperature at 15 cm depth	22°C	22.5°C	27.5°C
Soil temperature at 30 cm depth	23.5°C	21.5°C	-
Soil temperature at 45 cm depth	24°C	23°C	-

city. It can be noticed that the crop temperature decreased from Jan. 5, 1997 to Feb. 11, 1997. This confirms the inverse relationship between NDVI and surface temperature over vegetation region (Gupta *et al.*, 1997). On Feb. 28, 1997, the surface temperatures of the agriculture region surrounding Anand show higher temperatures as compared to those for Feb. 11, 1997, which is due to shift in the phenological stage of the crops towards maturity/senescence stage.

Consistency check for surface temperature data

Table 4 shows the land surface temperature derived from NOAA/AVHRR data for the pixel encompassing the tower location, on January 5, February 11 and February 28, 1997 together with corresponding in situ agrometeorological

measurements and surface-based radiometric temperature measurements. Surface meteorological observations, the soil temperature at 2 cm depth (surrogate to surface temperature), 5, 10, 15, 30 and 45 cm depths were recorded at the GAU Observatory, Anand.

On Jan. 5, 1997 radiometric crop temperature was 21°C, while the soil temperature at 2 cm depth was 43°C. The ST derived from NOAA/AVHRR was 28.8°C, which is relatively nearer to crop temperature (21°C) compared to that for soil temperature at 2 cm depth (43°C) as the canopy was fully developed. The NDVI value for the pixel encompassing the tower location on Jan. 5, 1997 was 0.385 which reached highest value of 0.4 on Feb. 11, 1997 and thereafter decreased to 0.254 on Feb. 28, 1997

(Table 5) and this supports the fact that the crop canopy cover was very high on Jan.5 as well as on Feb. 11, 1997 and the crops were entering maturity/senescence stage by Feb. 28,

1997.

The NOAA/AVHRR derived ST on Feb. 11, 1997 was 30.1°C which is nearer to crop

Table 5: Surface temperature and NDVI derived from NOAA/AVHRR for three dates

(a) January 5, 1997

	1	2	3	4	5	6
1	27.44 0.422	27.56 0.458	26.22 0.486	26.01 0.472	31.54 0.303	31.92 0.283
2	26.60 0.477	26.63 0.482	26.4 0.482	30.45 0.352	30.68 0.328	33.87 0.225
3	27.95 0.441	26.06 0.477	28.83 0.385	28.34 0.383	28.21 0.373	27.42 0.392
4	28.91 0.340	26.69 0.450	26.53 0.440	26.69 0.469	25.41 0.487	25.28 0.492
5	27.11 0.419	28.17 0.394	27.98 0.394	28.0 0.394	27.47 0.419	28.17 0.394
6	28.42 0.371	28.7 0.345	28.45 0.338	26.92 0.400	27.52 0.392	28.71 0.361

(b) February 11, 1997

	1	2	3	4	5	6
1	28.63 0.472	28.36 0.501	28.97 0.472	28.26 0.497	29.23 0.460	26.61 0.540
2	29.82 0.492	29.08 0.476	28.43 0.488	29.70 0.440	31.34 0.369	31.95 0.303
3	28.02 0.500	26.82 0.515	30.15 0.400	30.04 0.425	30.723 0.400	5.830 0.243
4	26.46 0.515	28.11 0.473	28.17 0.469	29.64 0.393	31.38 0.308	29.85 0.341
5	26.48 0.498	26.92 0.481	26.50 0.493	25.37 0.518	24.45 0.537	25.72 0.525
6	26.56 0.501	27.20 0.461	26.41 0.485	26.66 0.477	28.44 0.469	29.16 0.456

Table 5: Contd...

(c) February 28, 1997

	1	2	3	4	5	6
1	43.94 0.264	40.27 0.259	40.27 0.373	43.48 0.311	42.36 0.311	40.79 0.373
2	39.03 0.420	40.97 0.400	41.89 0.377	43.58 0.262	40.45 0.365	40.47 0.380
3	42.71 0.357	43.08 0.361	43.36 0.254	41.07 0.350	38.63 0.381	37.93 0.402
4	41.64 0.336	42.13 0.339	39.23 0.379	35.02 0.452	33.55 0.467	36.25 0.432
5	39.42 0.374	39.17 0.374	38.13 0.407	35.93 0.440	37.69 0.430	40.40 0.386
6	40.88 0.324	40.71 0.324	40.88 0.365	43.04 0.368	44.10 0.350	42.07 0.376

temperature as compared to soil temperature at 2 cm depth. The NDVI for the two dates (Jan. 5 and Feb. 11, 1997) was nearly same [0.385 for Jan. 5, 1997 and 0.4 for Feb. 11, 1997, please see Table 5(a) and (b)] and for this reason the ST for the pixel for these two dates was similar. It may be noted that practically there was no significant change in air temperature on these two dates (Table 4). High NDVI value indicates the dominant contribution of crop and for this reason, the surface temperatures obtained from AVHRR were weighted more towards crop temperature as compared to that for soil temperature at 2 cm depth.

On Feb. 26, 1997, radiometric crop temperature was 32.4°C and soil temperature at 2 cm depth was 45.3°C. At this time, the crops were nearing maturity/senescence stage [NDVI got reduced, please see Table 5(c)]. This is further supported by the fact that the difference between crop temperature and air

temperature was small (0.6°C) on Feb. 26, 1997 as compared to 1.4°C and 6.2°C on Feb. 11/12, 1997 and Jan. 5, 1997, respectively. The ST derived from NOAA/AVHRR data of Feb. 26, 1997 was 40°C and that on Feb. 28, 1997 was 43°C. As the crops in the region have reached maturity/senescence stage and due to harvesting, the NOAA/AVHRR ST on Feb. 26 was contributed more by soil than that of crops.

Table 5 shows surface temperature and NDVI of the pixel encompassing the LSP tower (identified by rectangular enclosure) and also for surrounding pixels together with the corresponding NDVI values. Further, temperature variations for these dates were also examined together with the NDVI values. On Jan. 5, 1997, in the directions of north to west of the tower location [i.e., the pixels (1,1), (1,2), (1,3), (2,1), (2,2), (2,3), (3,1) and (3,2), where the first number in the bracket

refers to the row number and the second to the column number], NDVI values are higher than that of the pixel encompassing the tower and the temperatures are lower by 0.88-2.76°C. Visual examination of the AVHRR data showed that this is due to intense cultivation in these directions.

In the east and northeast direction (excluding pixel (1,4)), NDVI values were lower or comparable with that for the pixel encompassing the tower.

As expected, the surface temperature values were becoming higher in case of pixels with considerably lower NDVI values as compared to that of the pixel encompassing the tower location. This may be due to mix up of different types of land cover in the pixels (referred to as mixed pixels).

In the south, southeast and southwest directions, the NDVI values were comparable (temperatures also comparable) and more in southeast direction (temperatures lower than that of the pixel encompassing the tower). The increase in NDVI values in these pixels is due to intense cultivation practice.

Since all crops were in reproductive stage by Feb. 11, 1997, higher (or comparable) values of NDVI were observed in all directions (Table 5(b)) with reference to NDVI observed on Jan. 5, 1997 (Table 5(a)) except for pixels at (3, 6) and (4, 6) which showed a decrease in the values of NDVI (with a corresponding increase in surface temperature) with reference to Jan. 5, 1997. This may be due to high altitude cirrus clouds, which would not get detected in 1.1 km resolution AVHRR data. Due to seasonal change, surface temperatures were, in general, higher for all the pixels. Further, the response of NDVI is

nearly flat during peak vegetative through maturity/senescence stages. Thus during these stages the sensitivity levels of NDVI and surface temperatures will not match, which is also responsible for not getting well defined opposite phase patterns in the temporal trends of surface temperatures and NDVIs.

By Feb. 28, 1997 the crops were reaching maturity/senescence stage. With reference to Table 5(c), but for a few pixels [(4,4), (4,5) and (4,6)] NDVI decreased on Feb. 28, 1997 as compared to those on Feb. 11, 1997. For some pixels, still significantly high value of NDVI on Feb. 28, 1997 indicates that the crops in these areas were still reaching maturity rather than having reached maturity. Here, decrease in NDVI was accompanied with an increase in temperature as expected during maturity/senescence stage. Increase in ST for the pixel encompassing the LSP tower and the GAU Observatory region from Feb. 11, 1997 to Feb. 28, 1997 (Table 4) was 32.7% (9°C). An increase of near similar magnitude would also be present in the other pixels and that accounts for the difference in trend between ST and NDVI when the parameters for the two dates are compared.

Estimation of sensible heat flux (SHF) from AVHRR data

In order to calculate SHF, the resistance to heat exchanges (r) need to be estimated using eq. (10). For this computation Z was assumed to be -3.12 m (i.e., average of geometric mean of possible combinations of 1, 2, 4 and 8 m referring to different levels of LSP tower).

Plate 10 shows the sensible heat flux image for the Anand region computed using the ST

and Z_0 obtained from NOAA AVHRR following Vining and Blad (1992). Air temperature from the observatory and friction velocity (u^*) was provided by IITM. As can be expected, sensible heat flux was very high ($700-1009 \text{ Wm}^{-2}$) where vegetation is sparse in the direction far-west and far south to Anand, whereas, the flux values are in the range of $200-500 \text{ Wm}^{-2}$ in the areas having extensive crops. The conventional measurement of sensible heat flux over the GAU observatory at 1330 hrs. was found to be 214.06 Wm^{-2} and the satellite at the tower location yielded a value of 215.19 Wm^{-2} . The magnitude of SHF over certain agriculture region is relatively high as the crops were entering into maturity/senescence stage.

CONCLUSIONS

Roughness length

Table 6 gives the information on the comparison aspect of estimated Z_0 from methods based on A (page 197) from AVHRR data and wind profile method while Table 7 addresses to this aspect with reference to WiFS data. The 1100 m resolution AVHRR pixel will have about 5.85 WiFS pixels of 188 m resolution. Thus 13 AVHRR pixels need to correspond to 76 WiFS pixels. The standard error could be 5.85 pixels. Thus 13 AVHRR pixels could be equivalent to 82 WiFS pixels. As scan angle geometry for WiFS and AVHRR would not be the same, one could expect some add-on WiFS pixels for working out the correspondence with the distance in terms of AVHRR pixels. Consistency in the location modes in AVHRR and WiFS have a large mismatch for methods A(ii) and A(iii) and due to this the percentage error in the estimation of Z_0 by these methods are higher for WiFS as compared to estimations from AVHRR data.

The wide spread nature of mode for methods A(ii) and A(iii) looks to be the primary reason for it. Thus the methods A(ii) and A(iii) could not be considered reliable for semi-operational application.

For circular average method A(i), the distance of mode for Z_0 in the case of AVHRR as well as WiFS was matching and mode was also uniquely defined (was not widespread). Further, the circular average method could be representative of a wide spread region and for estimating a single value for the daytime (due to high variability in wind direction).

The degree of mismatch in Z_0 estimated with wind profile method and AVHRR data (4.4%) and WiFS data (-2.6%) were within the tolerable limits besides being consistent with reference to distance of mode (for Z_0) from tower for AVHRR as well as WiFS data sets. Thus this method, i.e., A(i) is reliable.

The method B using AVHRR and WiFS data overestimated the value of Z_0 with reference to Z_0 computed by wind profile method (using tower-based measurements). Thus this method is also not reliable.

Surface temperature

Surface temperature estimated for pixel encompassing the tower from AVHRR data (Feb. 26, 1997) was about 40°C . Areas having good vegetation cover showed lower temperature than barren areas, which is expected. This proves that the surface temperature derived from AVHRR data is consistent and thus reliable.

Sensible heat flux

Estimation of sensible heat flux has good promise in the case of the NOAA/AVHRR data.

Table 6: Comparison of Z_0 estimated from AVHRR data for methods A(i), A(ii) and A(iii) with wind profile data for Feb. 26, 1997

Method	Estimated Z_0 from AVHRR data (m)	Percentage difference between AVHRR Z_0 and $Z_0=0.2692$ m from wind profile method	Distance from tower pixel for AVHRR data-based Z_0 (in terms of number of AVHRR pixels)
A(i): Circular average	0.2811	4.4	13
A(ii): for average in 15°-30° sector	0.2697	0.02	12
A(iii): ±1° w.r.to 27° wind direction	0.2604	-3	13

Table 7: Comparison of Z_0 estimated from WiFS data for methods A(i), A(ii) and A(iii) with wind profile data for Feb. 25, 1997

Method	Estimated Z_0 from WiFS (m)	Percentage difference between WiFS Z_0 and $Z_0=0.2972$ m from wind profile method	Distance from tower pixel for WiFS data-based Z_0 (in terms of number of WiFS pixels)
A(i): Circular average	0.2893	-2.6	86
A(ii): for average in 15°-30° sector	0.3313	11.0	43
A(iii): ±1° w.r.to 27° wind direction	0.3187	7.2	44

In this case, the conventionally measured value was 214.06 Wm^{-2} while the satellite derived value was 215.19 Wm^{-2} . This good matching could also be a coincidence. Here, further work with the Intensive Observation Period (IOP) data sets from IITM would enable development of operational/semi-operational level algorithms.

SCOPE FOR FURTHER WORK

To obtain more accurate results, equations relating roughness length and NDVI must be worked out for Indian conditions. This involves use of multi-temporal data. For obtainment of realistic NDVI from NOAA/AVHRR data, the radiances were first corrected for scan angle

effects using dark body method. This approach, although a very good approximation, may not be the *correct* one. The latest sensors on board Terra satellite such as MODIS, which provide information about the state of the atmosphere at the time of data acquisition itself, would enable better atmospheric corrections.

Since estimation of roughness length using NDVI is relevant only for areas covered with vegetation, for areas devoid of vegetation, new method must be worked out. One way to overcome this problem could be to incorporate standard values of conventional roughness length and use NDVI based roughness length over non-urban areas. For this, Geographical Information System (GIS) may become a tool of high utility in achieving this mix-up.

ACKNOWLEDGEMENTS

The authors thank Dr. D.P. Rao, former Director, National Remote Sensing Agency (NRSA), Dr. R.R. Navalgund, Director, NRSA and Prof. S.K. Bhan, Dy. Director (Applications), NRSA for permitting to pursue this study and publish it. Authors are grateful to Mr. M.V. Rao and Mr. K.H. Rao of NRSA for their help during the research by providing AVHRR data in a timely manner. Authors thank Mr. S. Sinha, Mr. Brij Mohan, Mr. B.S. Murthy and Mr. K.G. Vernekar of Indian Institute of Tropical Meteorology (IITM), Pune and Mr. J.S. Pillai (formerly of IITM and now with SAMEER) for having been helpful in providing initial LASPEX data sets and converging discussions. Managerial cares provided by Dr. G.B. Pant, Director, IITM are gratefully acknowledged. Help provided by Mrs. A.A. Shiralkar of IITM through timely transmission of requested literature is also thankfully acknowledged. Authors feel indebted to Prof. A.M. Sheikh, Prof. M.B.

Savani and Dr. V. Pandey for providing the data containing wind-direction, air temperature etc. and for providing help during the NRSA field experiment at Anand. The secretarial support provided by Mr. Ramesh Babu is thankfully acknowledged.

REFERENCES

- Bannari, A., Morin, D. and Bonn, F. 1995. A review of Vegetation Indices. *Rem. Sens. Rev.*, 13 : 95-120.
- Becker, F. and Li, Z. L. 1990. Towards a local split window method over land surface. *Int. J. Rem. Sens.*, 11 : 369-393.
- Bolle, H. J. and Streckenbach, B. (eds.), 1993. Flux estimates from remote sensing. The echival field experiment in a desertification threatened area (EFEDA) final report. pp. 406-424, Berlin, August.
- Chehbouni, A., Nichols, W. D., Njoku, E. G., Qi, J., Kerr, Y. H. and Cabot, F. 1997. A three component model to estimate sensible heat flux over sparse shrubs in Nevada. *Rem. Sens. Rev.*, 15:99-112.
- Deekshatulu, B. L. and Gupta, R. K. 1994. remote sensing and vegetation. *Proc. Indian. Nat. Sci. Acad.*, 60(1) : 299-333.
- Gupta, R. K., Prasad, S., Sessa Sai, M. V. R. and Viswanadham, T. S. 1997. The estimation of surface temperature over an agricultural area in the state of Haryana and Punjab, India and its relationship with the normalized difference vegetation index (NDVI) using NOAA-AVHRR data. *Int. J. Rem. Sens.*, 18(18) : 3729-3741.
- Hall, F. G., Heumrich, K. F., Goetz, S. J., Sellers, P. J. and Nickenson, J. E. 1992.

- satellite remote sensing of surface Energy balance : Successes, Failures and Unresolved issues of FIFE. *J. Geophys. Res.*, 97(D17): 19061-19089.
- Rao, C. R. N. and Chen, J. 1996. Post-launch calibration of the visible and near-infrared channels of the advanced very high resolution radiometer on the NOAA-14 spacecraft. *Int. J. Rem. Sens.*, 17(14) : 2743-2747.
- Vining, R. C. and Blad, B. L. 1992. Estimation of sensible heat flux from remotely sensed canopy temperatures. *J. Geophys. Res.*, 97 (D17) : 18951 -18954.